INTERNATIONAL JOURNAL OF
NUMERICAL ANALYSIS AND MODELING
Volume 13, Number 5, Pages 753–762

THE UNSTABLE MODE IN THE CRANK-NICOLSON LEAP-FROG METHOD IS STABLE

NICK HURL, WILLIAM LAYTON, YONG LI, AND MARINA MORAITI

Abstract. This report proves that under the time step condition $\Delta t|\Lambda| < 1$ ($|\cdot|$ = Euclidean norm) suggested by root condition analysis and necessary for stability, all modes of the Crank-Nicolson Leap-Frog (CNLF) approximate solution to the system

$$\frac{du}{dt} + Au + \Lambda u = 0, \text{ for } t > 0 \text{ and } u(0) = u_0,$$

where $A + A^T$ is symmetric positive definite and Λ is skew symmetric, are asymptotically stable. This result gives a sufficient stability condition for non-commutative A and Λ, and is proven by energy methods. Thus, the growth, often reported in the unstable mode, is not due to systems effects and its explanation must be sought elsewhere.

Key words. IMEX method, Crank-Nicolson Leap-Frog, CNLF, unstable mode, computational mode.

1. Introduction

Implicit-explicit (IMEX) time-stepping schemes are often used for solving multi-physics problems with both stiff and nonstiff components, e.g., advection-diffusion-reaction equations, Navier-Stokes equations, geophysical flows, surface-groundwater flows. IMEX schemes treat the stiff term implicitly and the nonstiff term explicitly, and thus suffer from neither the computational expense of fully implicit schemes nor the demanding time step requirement of fully explicit methods, e.g., [1, 6, 7, 23].

The Crank-Nicolson Leap-Frog (CNLF) scheme, a classic two-step IMEX method, is frequently used in atmospheric flow simulations [1, 6, 17]. In this article, we prove asymptotic stability of the *unstable* or *computational mode* of the CNLF method for the system

$$\frac{du}{dt} + Au + \Lambda u = 0, \text{ for } t > 0 \text{ and } u(0) = u_0, \tag{1}$$

where $A_s = \frac{1}{2}(A + A^T) > 0$ (A_s is symmetric positive definite) and Λ is skew symmetric. Here $u : [0, \infty) \to \mathbb{R}^d$ and the square, *non-commutative*, real matrices A, Λ have compatible dimensions. Under these conditions, the solution to (1) satisfies $u(t) \to 0$ as $t \to \infty$, so any growth in the approximate solution is a numerics induced instability. With superscript denoting the time step number, CNLF, the IMEX combination of Crank-Nicolson and Leap-Frog, is given by: given u^0, u^1, find u^{n+1} satisfying for $n \geq 1$:

$$\frac{u^{n+1} - u^{n-1}}{2\Delta t} + A\frac{u^{n+1} + u^{n-1}}{2} + \Lambda u^n = 0. \tag{CNLF}$$

Received by the editors April 22, 2015 and, in revised form, September 11, 2015.
2000 *Mathematics Subject Classification.* 65.
The research of the authors was partially supported by the NSF under grants DMS-1216465 and DMS-1522267, and by AFOSR under grant FA 9550-12-1-0191.

Root condition analysis of CNLF for the scalar test problem $y' + ay + i\lambda y = 0$ leads to the necessary time step condition essentially from [11]:

$$\Delta t|\Lambda| < 1, \quad |\cdot| = \text{Euclidean norm.} \tag{2}$$

This condition was recently proven (by discrete energy methods) sufficient for stability in [15].

However, in practical simulations, difficulties with CNLF's unstable mode occur. It is often reported (see for example [5], [12], [19], [2], [18], [22], [10]) that as $n \to \infty$,

$$\begin{aligned} &\text{Stable Mode: } |u^{n+1} + u^{n-1}| \to 0, \\ &\text{Unstable Mode: } |u^{n+1} - u^{n-1}| \to \infty. \end{aligned} \tag{3}$$

CNLF is used for many geophysical flow simulations from which experience with and fixes for the unstable mode are correspondingly large, e.g., [5], [12], [13], [19], [2], [18], [22], [10]. One mystery is that since CNLF is stable under (2), no growth is possible in theory and yet time filters to deal with (3) are nearly universal in practice, [10, 16, 22]. It is an open question to determine if this could be due to the gap for IMEX methods (e.g., [1], [3], [6], [8], [20], [21]) between necessary conditions from root condition analysis and sufficient ones for systems, to roundoff errors exciting the weak instability in LF not sufficiently damped by CN, to imperfect imposition of (2), to nonlinearities or other unknown causes.

We prove that under (2) *the CNLF unstable mode is asymptotically stable* for the system (1). This result, consistent with numerical tests in Section 3, supports the scenario that growth in the unstable mode is not due to a system effect but rather due to imperfect imposition of and thus slight violation of (2), or non-autonomous effects studied in [14], or the combination of roundoff errors breaking skew symmetry in Λ and near singularity of A.

Theorem 1. *Consider (CNLF) for non-commutative A, Λ. Suppose the (necessary) time step condition (2) holds. Then, all modes of CNLF are asymptotically stable:*

$$u^n \to 0 \text{ as } n \to \infty \text{ and thus both}$$
$$u^{n+1} + u^{n-1} \to 0 \text{ and } u^{n+1} - u^{n-1} \to 0.$$

Remark 2. *If the matrices A and Λ commute then this follows from standard root condition analysis. Thus, (2) is a* necessary *condition for asymptotic stability. For single linear multistep methods it is known that root conditions are also sufficient. However, for implicit-explicit combinations of different methods, such as CNLF, root conditions are* not sufficient. *For example, Asher, Ruuth and Wetton* [1] *page 811 note "these results provide necessary but not sufficient conditions for stability..." and Hundsdorfer and Ruuth* [7] *page 2019 note "Theoretical results are difficult to obtain if these linearizations do not commute...". The only general path (that we take in Section 2) to a sufficient condition for systems is through energy methods.*

2. Three examples of the structure (1)

It is very common for problems in applications to have the structure of (1), a dissipative perturbation of a conservative system. We give three simple examples.

2.1. Transport plus diffusion. Suppressing spacial discretization, suppose we take $Au = -\epsilon u_{xx}$ (typically ϵ is small). Then (1) becomes the evolutionary convection-diffusion problem:

$$\frac{\partial u}{\partial t} - \epsilon \frac{\partial^2 u}{\partial x^2} + c\frac{\partial u}{\partial x} = 0, \quad -\infty < x < \infty,\ t > 0. \tag{4}$$

The CNLF method for (4) is to find u^{n+1} given u^n and u^{n-1}, satisfying, for all $n \geq 1$:

$$\frac{u^{n+1} - u^{n-1}}{2\Delta t} - \epsilon \frac{\partial^2}{\partial x^2}\left(\frac{u^{n+1} + u^{n-1}}{2}\right) + c\frac{\partial u^n}{\partial x} = 0.$$

2.2. Stokes flow plus Coriolis force. The use of (CNLF) in geophysical flows is based on fast-slow wave decompositions and time filters, see [19], [22]. Let Ω be a 2 or 3-dimensional bounded regular domain, u denote the velocity, p the pressure, f the body forces, and ν the kinematic viscosity. Omitting many of the complexities in geophysics, the system representing Stokes flow plus a Coriolis force, $f_C \times u$, is:

$$u_t - \nu\Delta u + \nabla p + f_C \times u = f(x,t), \text{ and } \nabla \cdot u = 0 \text{ in } \Omega,$$
$$u = 0 \text{ on } \partial\Omega, \text{ and } u(x,0) = u_0(x) \text{ in } \Omega.$$

We assume conforming velocity-pressure finite element spaces, $X^h \subset \left(H_0^1(\Omega)\right)^d$ and $Q^h \subset L_0^2(\Omega)$, satisfying the usual discrete inf-sup condition for stability of the discrete pressure, and denote the usual L^2 inner product over Ω by $(\cdot,\cdot)$. Letting $\Lambda u := f_C \times u$, the (CNLF) realization is to find $(u_h^{n+1}, p_h^{n+1}) \in X^h \times Q^h$, given $u_h^n, u_h^{n-1} \in X^h$, satisfying, for all $(v_h, q_h) \in X^h \times Q^h$ and all $n \geq 1$:

$$\left(\tfrac{u_h^{n+1} - u_h^{n-1}}{2\Delta t}, v_h\right) + \nu\left(\nabla\left(\tfrac{u_h^{n+1} + u_h^{n-1}}{2}\right), \nabla v_h\right) + (\Lambda u_h^n, v_h)$$
$$-\left(\tfrac{p_h^{n+1} + p_h^{n-1}}{2}, \nabla \cdot v_h\right) + \left(q_h, \nabla \cdot \left(\tfrac{u_h^{n+1} + u_h^{n-1}}{2}\right)\right) = (f^n, v_h).$$

2.3. The evolutionary Stokes-Darcy problem. Consider the application of (CNLF) to the uncoupling of surface and groundwater flows. Let Ω_f and Ω_p be 2 or 3-dimensional bounded regular domains that lie across an interface, I. The fluid velocity, u, fluid pressure, p, and hydraulic head, ϕ, satisfy the Stokes and the groundwater flow equations:

$$\begin{gathered} u_t - \nu\Delta u + \nabla p = f_f(x,t), \nabla \cdot u = 0, \text{ in } \Omega_f, \\ S_0\phi_t - \nabla \cdot (\mathcal{K}\nabla\phi) = f_p(x,t), \text{ in } \Omega_p, \\ \phi(x,0) = \phi_0(x), \text{ in } \Omega_p \text{ and } u(x,0) = u_0(x), \text{ in } \Omega_f, \\ \phi(x,t) = 0, \text{ in } \partial\Omega_p \backslash I \text{ and } u(x,t) = 0, \text{ in } \partial\Omega_f \backslash I. \end{gathered} \tag{5}$$

Let $\widehat{n}_{f/p}$ denote the outward unit normal vector on I associated with $\Omega_{f/p}$ and $\widehat{\tau}_i$ denote an orthonormal basis of tangent vectors on I. The coupling conditions across I are conservation of mass, balance of forces and the Beavers-Joseph-Saffman condition on the tangential velocity:

$$u \cdot \widehat{n}_f - \mathcal{K}\nabla\phi \cdot \widehat{n}_p = 0 \text{ and } p - \nu\ \widehat{n}_f \cdot \nabla u \cdot \widehat{n}_f = g\phi \text{ on } I,$$
$$-\nu\ \nabla u \cdot \widehat{n}_f = \tfrac{\alpha_{\mathrm{BJS}}}{\sqrt{\widehat{\tau}_i \cdot \mathcal{K}\widehat{\tau}_i}} u \cdot \widehat{\tau}_i \text{ on } I, \text{ for any } \widehat{\tau}_i \text{ tangent vector on } I.$$

Here, g, $\mathcal{K}$, ν and S_0 are the gravitational acceleration constant, hydraulic conductivity tensor, kinematic viscosity and specific mass storativity coefficient, respectively, all positive. We denote by $(\cdot,\cdot)_{f/p}$ the L^2 inner product over $\Omega_{f/p}$.

To discretize the Stokes-Darcy problem in space by the finite element method, we choose conforming velocity, pressure, and hydraulic head spaces:

$$\begin{aligned}
\text{Velocity} &: \quad X_f^h \subset \{v \in \left(H^1(\Omega_f)\right)^d : v = 0 \text{ on } \ \partial\Omega_f \backslash I\},\\
\text{Pressure} &: \quad Q_f^h \subset L^2(\Omega_f),\\
\text{Hydraulic Head} &: \quad X_p^h \subset \{\psi \in H^1(\Omega_p) : \psi = 0 \text{ on } \ \partial\Omega_p \backslash I\},
\end{aligned}$$

and X_f^h and Q_f^h are assumed to satisfy the discrete inf-sup condition. Letting

$$\begin{aligned}
a_f(u,v) &:= \nu(\nabla u, \nabla v)_f + \sum_i \int_I \tfrac{\alpha_{\rm BJS}}{\sqrt{\widehat{\tau}_i \cdot \mathcal{K}\widehat{\tau}_i}} (u\cdot\widehat{\tau}_i)(v\cdot\widehat{\tau}_i)\ ds,\\
a_p(\phi,\psi) &:= g(\mathcal{K}\nabla\phi, \nabla\psi)_p, \quad \text{and}\\
c_I(u,\phi) &:= g\int_I \phi u \cdot \widehat{n}_f\ ds,
\end{aligned}$$

the (CNLF) method for Stokes-Darcy is to find $(u_h^{n+1}, p_h^{n+1}, \phi_h^{n+1}) \in X_f^h \times Q_f^h \times X_p^h$, given (u_h^n, p_h^n, ϕ_h^n), $(u_h^{n-1}, p_h^{n-1}, \phi_h^{n-1}) \in X_f^h \times Q_f^h \times X_p^h$ satisfying $\forall\ (v_h, q_h, \psi_h) \in X_f^h \times Q_f^h \times X_p^h$:

$$\begin{gathered}
\left(\tfrac{u_h^{n+1}-u_h^{n-1}}{2\Delta t}, v_h\right)_f + a_f\left(\tfrac{u_h^{n+1}+u_h^{n-1}}{2}, v_h\right) - \left(\tfrac{p_h^{n+1}+p_h^{n-1}}{2}, \nabla\cdot v_h\right)_f\\
+c_I(v_h, \phi_h^n) = (f_f^n, v_h)_f\\
(q_h, \nabla\cdot u_h^{n+1})_f = 0,\\
gS_0\left(\tfrac{\phi_h^{n+1}-\phi_h^{n-1}}{2\Delta t}, \psi_h\right)_p + a_p\left(\tfrac{\phi_h^{n+1}+\phi_h^{n-1}}{2}, \psi_h\right) - c_I(u_h^n, \psi_h) = g(f_p^n, \psi_h)_p.
\end{gathered}$$

3. Proof of asymptotic stability of the unstable mode

This section gives a direct energy proof of Theorem 1.1. Let $A_s = \frac{1}{2}(A + A^T), A_{sk} = \frac{1}{2}(A - A^T)$. Denote the usual Euclidean inner product and norm by $\langle w, v\rangle := w^T v$, $|v|^2 := \langle v, v\rangle$ and the $A-$norm (well defined since $A_s > 0$) by

$$|u|_A^2 := u^T A u = u^T A_s u = \langle A_s u, u\rangle\,.$$

Step 1: Energy stability. In step 1 we follow [15]. Take the inner product of CNLF with $u^{n+1} + u^{n-1}$, add and subtract $|u^n|^2$ and multiply through by $2\Delta t$. This yields

$$\begin{gathered}
\left[|u^{n+1}|^2 + |u^n|^2\right] - \left[|u^n|^2 + |u^{n-1}|^2\right]\\
+\Delta t|u^{n+1} + u^{n-1}|_A^2 + 2\Delta t\langle \Lambda u^n, u^{n+1} + u^{n-1}\rangle = 0.
\end{gathered} \tag{6}$$

Next, using skew symmetry, rearrange to get

$$2\Delta t\langle \Lambda u^n, u^{n+1} + u^{n-1}\rangle = 2\Delta t\langle \Lambda u^n, u^{n+1}\rangle - 2\Delta t\left\langle \Lambda u^{n-1}, u^n\right\rangle.$$

Define the first energy (which is positive if $\Delta t|\Lambda| < 1$, [15])

$$E^{n+1/2} := |u^{n+1}|^2 + |u^n|^2 + 2\Delta t\langle \Lambda u^n, u^{n+1}\rangle.$$

Collecting terms we obtain

$$E^{n+1/2} - E^{n-1/2} + \Delta t|u^{n+1} + u^{n-1}|_A^2 = 0. \tag{7}$$

This implies that the stable mode $u^{n+1} + u^{n-1} \to 0$ as $n \to \infty$. Indeed, summing for $n = 1, \cdots, N$ and then letting $N \to \infty$, we see that

$$\sum\nolimits_{n=1}^{\infty} |u^{n+1} + u^{n-1}|_A^2 < \infty$$

and thus the n^{th} term $|u^{n+1}+u^{n-1}|_A^2 \to 0$.

Step 2: The key estimate. Take the inner product of CNLF with $u^{n+1}-u^{n-1}$ and multiply through by $2\Delta t\delta$ where $\delta>0$ will be determined later. This gives

$$\begin{aligned}&\Delta t\delta\left\langle A(u^{n+1}+u^{n-1}),u^{n+1}-u^{n-1}\right\rangle\\ &+\delta|u^{n+1}-u^{n-1}|^2+2\delta\Delta t\langle\Lambda u^n,u^{n+1}-u^{n-1}\rangle=0.\end{aligned}\tag{8}$$

Split the operator $A=A_s+A_{sk}$. The first term of (8) becomes

$$\begin{aligned}&\left\langle A(u^{n+1}+u^{n-1}),u^{n+1}-u^{n-1}\right\rangle\\ &=\left\langle A_s(u^{n+1}+u^{n-1}),u^{n+1}-u^{n-1}\right\rangle+\left\langle A_{sk}(u^{n+1}+u^{n-1}),u^{n+1}-u^{n-1}\right\rangle\\ &=\left\langle A_su^{n+1},u^{n+1}\right\rangle-\left\langle A_su^{n-1},u^{n-1}\right\rangle+\left\langle A_{sk}(u^{n+1}+u^{n-1}),u^{n+1}-u^{n-1}\right\rangle\\ &=|u^{n+1}|_A^2-|u^{n-1}|_A^2+\left\langle A_{sk}(u^{n+1}+u^{n-1}),u^{n+1}-u^{n-1}\right\rangle.\end{aligned}$$

Use the above equality for the first term in (8) and add and subtract $\Delta t\delta|u^n|_A^2$ to obtain

$$\begin{aligned}&\left[\delta\Delta t|u^{n+1}|_A^2+\delta\Delta t|u^n|_A^2\right]-\left[\delta\Delta t|u^n|_A^2+\delta\Delta t|u^{n-1}|_A^2\right]\\ &+\delta\Delta t\left\langle A_{sk}(u^{n+1}+u^{n-1}),u^{n+1}-u^{n-1}\right\rangle\\ &+\delta|u^{n+1}-u^{n-1}|^2+2\delta\Delta t\langle\Lambda u^n,u^{n+1}-u^{n-1}\rangle=0.\end{aligned}\tag{9}$$

Define the second energy

$$\mathcal{E}^{n+1/2}:=E^{n+1/2}+\delta\Delta t|u^{n+1}|_A^2+\delta\Delta t|u^n|_A^2.$$

The *key step* is adding (7) and (9) which gives

$$\begin{aligned}&\mathcal{E}^{n+1/2}-\mathcal{E}^{n-1/2}+\Delta t|u^{n+1}+u^{n-1}|_A^2+\delta|u^{n+1}-u^{n-1}|^2\\ &+\delta\Delta t\left\langle A_{sk}(u^{n+1}+u^{n-1}),u^{n+1}-u^{n-1}\right\rangle+2\delta\Delta t\langle\Lambda u^n,u^{n+1}-u^{n-1}\rangle=0.\end{aligned}$$

Summing this from $n=1$ to N gives

$$\mathcal{E}^{N+1/2}+\sum_{n=1}^{N}\left[\Delta t|u^{n+1}+u^{n-1}|_A^2+\delta|u^{n+1}-u^{n-1}|^2\right]+Q_1+Q_2=\mathcal{E}^{1/2},\tag{10}$$

$$Q_1:=\sum_{n=1}^{N}\delta\Delta t\left\langle A_{sk}(u^{n+1}+u^{n-1}),u^{n+1}-u^{n-1}\right\rangle,$$

$$Q_2:=\sum_{n=1}^{N}2\delta\Delta t\langle\Lambda u^n,u^{n+1}-u^{n-1}\rangle.$$

Step 3: Bounding $|Q_1|$ & $|Q_2|$. For Q_1 note that

$$\begin{aligned}\left\langle A_{sk}(u^{n+1}+u^{n-1}),u^{n+1}-u^{n-1}\right\rangle&\le|A_{sk}||u^{n+1}+u^{n-1}||u^{n+1}-u^{n-1}|\\ &\le\frac{1}{2\epsilon}|A_{sk}||u^{n+1}+u^{n-1}|^2+\frac{\epsilon}{2}|A_{sk}||u^{n+1}-u^{n-1}|^2\end{aligned}$$

where $\epsilon>0$. Hence

$$|Q_1|\le\sum_{n=1}^{N}\frac{\delta\Delta t}{2\epsilon}|A_{sk}||u^{n+1}+u^{n-1}|^2+\sum_{n=1}^{N}\frac{\delta\Delta t\epsilon}{2}|A_{sk}||u^{n+1}-u^{n-1}|^2.$$

For Q_2 note that

$$\begin{aligned}
&\langle \Lambda u^n, u^{n+1} - u^{n-1} \rangle = \\
&= \frac{1}{2}\langle \Lambda(u^n - u^{n-2}), u^{n+1} - u^{n-1} \rangle + \frac{1}{2}\langle \Lambda(u^n + u^{n-2}), u^{n+1} - u^{n-1} \rangle \\
&\le \frac{1}{2}|\Lambda||u^n - u^{n-2}||u^{n+1} - u^{n-1}| + \frac{1}{2}|\Lambda||u^n + u^{n-2}||u^{n+1} - u^{n-1}| \\
&\le \frac{1}{2}|\Lambda| \left(\frac{1}{2}|u^n - u^{n-2}|^2 + \frac{1}{2}|u^{n+1} - u^{n-1}|^2 \right) \\
&+ \frac{1}{2}|\Lambda| \left(\frac{1}{2\epsilon}|u^n + u^{n-2}|^2 + \frac{\epsilon}{2}|u^{n+1} - u^{n-1}|^2 \right). \qquad (11)
\end{aligned}$$

Then

$$\begin{aligned}
2\delta\Delta t \sum_{n=1}^{N} \frac{1}{2}|\Lambda| \left(\frac{1}{2}|u^n - u^{n-2}|^2 + \frac{1}{2}|u^{n+1} - u^{n-1}|^2 \right) &= \frac{\delta}{2}\Delta t|\Lambda||u^{N+1} - u^{N-1}|^2 + \\
+\delta\Delta t|\Lambda| \left(|u^N - u^{N-2}|^2 + \cdots + |u^3 - u^1|^2 \right) + \frac{\delta}{2}\Delta t|\Lambda||u^2 - u^0|^2 \\
\le \delta\Delta t|\Lambda| \sum_{n=1}^{N} |u^{n+1} - u^{n-1}|^2, \qquad (12)
\end{aligned}$$

and

$$\begin{aligned}
&2\delta\Delta t \sum_{n=1}^{N} \frac{1}{2}|\Lambda| \left(\frac{1}{2\epsilon}|u^n + u^{n-2}|^2 + \frac{\epsilon}{2}|u^{n+1} - u^{n-1}|^2 \right) = \\
&= \frac{\delta\Delta t|\Lambda|}{2\epsilon} \sum_{n=1}^{N-1} |u^{n+1} + u^{n-1}|^2 + \frac{\epsilon\delta\Delta t|\Lambda|}{2} \sum_{n=1}^{N} |u^{n+1} - u^{n-1}|^2 \\
&\le \frac{\delta\Delta t|\Lambda|}{2\epsilon} \sum_{n=1}^{N} |u^{n+1} + u^{n-1}|^2 + \frac{\epsilon\delta\Delta t|\Lambda|}{2} \sum_{n=1}^{N} |u^{n+1} - u^{n-1}|^2. \qquad (13)
\end{aligned}$$

Thus, $|Q_2|$ is now bounded by combining (12) and (13) as follows

$$|Q_2| \le \delta\Delta t|\Lambda| \left(1 + \frac{\epsilon}{2}\right) \sum_{n=1}^{N} |u^{n+1} - u^{n-1}|^2 + \frac{\delta\Delta t|\Lambda|}{2\epsilon} \sum_{n=1}^{N} |u^{n+1} + u^{n-1}|^2.$$

Hence

$$\begin{aligned}
|Q_1| + |Q_2| &\le \delta\Delta t \left(|\Lambda| \left(1 + \frac{\epsilon}{2}\right) + \frac{\epsilon}{2}|A_{sk}| \right) \sum_{n=1}^{N} |u^{n+1} - u^{n-1}|^2 \\
&+ \frac{\delta\Delta t}{2\epsilon} \Big(|\Lambda| + |A_{sk}| \Big) \sum_{n=1}^{N} |u^{n+1} + u^{n-1}|^2.
\end{aligned}$$

Step 4: Using the Q_1 & Q_2 estimates in the energy inequality. Inserting these estimates for Q_1 and Q_2 into the energy inequality and collecting terms gives

$$\begin{aligned}
&\mathcal{E}^{N+1/2} + \delta \left(1 - \left(1 + \frac{\epsilon}{2}\right)\Delta t|\Lambda| - \frac{\epsilon}{2}\Delta t|A_{sk}| \right) \sum_{n=1}^{N} |u^{n+1} - u^{n-1}|^2 \\
&+ \Delta t \sum_{n=1}^{N} \left(|u^{n+1} + u^{n-1}|_A^2 - \frac{\delta}{2\epsilon}\Big(|\Lambda| + |A_{sk}|\Big)|u^{n+1} + u^{n-1}|^2 \right) \le C(u^0, u^1). \qquad (14)
\end{aligned}$$

Step 5: Estimating the unstable mode. Since the RHS, $C(u^0, u^1)$, is independent of N, we can let $N \to \infty$ and conclude that

$$\delta\left(1-(1+\frac{\epsilon}{2})\Delta t|\Lambda| - \frac{\epsilon}{2}\Delta t|A_{sk}|\right)\sum_{n=1}^{\infty}|u^{n+1}-u^{n-1}|^2 +$$
$$+\Delta t\sum_{n=1}^{\infty}\left(|u^{n+1}+u^{n-1}|_A^2 - \frac{\delta}{2\epsilon}\left(|\Lambda|+|A_{sk}|\right)|u^{n+1}+u^{n-1}|^2\right) < \infty.$$

From this we shall deduce that $\sum_{n=1}^{\infty}|u^{n+1}-u^{n-1}|^2 < \infty$ and thus $|u^{n+1}-u^{n-1}|^2 \to 0$ as $n \to \infty$. To make this step, two conditions are required: the second sum must be non-negative and the coefficient of the first sum positive. That coefficient is positive if

$$\epsilon < 2\frac{1-\Delta t|\Lambda|}{\Delta t|\Lambda| + \Delta t|A_{sk}|}.$$

Since $\epsilon > 0$ is arbitrary, this condition can be satisfied if the stability condition $\Delta t|\Lambda| < 1$ holds. For the second sum to be non-negative, it suffices that

$$|u^{n+1}+u^{n-1}|_A^2 - \frac{\delta\left(|\Lambda|+|A_{sk}|\right)}{2\epsilon}|u^{n+1}+u^{n-1}|^2 \geq 0.$$

This can be attained by picking $\delta = \epsilon\lambda_{\min}(A_s)/\left(|\Lambda|+|A_{sk}|\right)$, where $\lambda_{\min}(A_s)$ denotes the minimum eigenvalue of A_s. With this condition on Δt and choice of δ, we conclude that the sum below converges:

$$\sum_{n=1}^{\infty}|u^{n+1}-u^{n-1}|^2 \leq C < \infty. \tag{15}$$

Thus the n^{th} term $|u^{n+1}-u^{n-1}|^2 \to 0$ and $|u^{n+1}+u^{n-1}|_A^2 \to 0$ from Step 1. Hence, $u^n \to 0$ and all modes, including the unstable mode, are controlled.

4. Numerical exploration of the unstable mode

The behavior of the unstable mode in practice is often associated with marginal stability (weak instability) of Leap-Frog. The first scenario we explore is thus as follows. Practical simulations often occur with many accompanying perturbations. Thus, the matrix Λ will only be skew symmetric to $\mathcal{O}(\varepsilon)$, where ε is the magnitude of the errors in numerical integration, computer arithmetic, function evaluation, previous calculations, and so on, used to generate Λ and form the product Λu. These perturb the eigenvalues of Λ to be outside the stability interval of Leap-Frog, $\{z : \mathrm{Re}(z) = 0, -1 < \mathrm{Im}(z) < +1\}$. CN contributes damping of the stable mode sufficient to control its growth. We test if these perturbations can cause the unstable mode's growth. The second scenario we test is whether slight violation of (2) (caused by computing near the CFL limit and imperfect estimation of $|\Lambda|$ due to these perturbations) is first seen in the unstable mode.

Test: Small perturbations of Λ. Let $A = \mathrm{diag}\{10^4, 10^{-4}\}$ and consider the 2×2 system

$$\frac{du}{dt} + 10^4 u + \varepsilon_1 u - v = 0, \ \frac{dv}{dt} + 10^{-4} v + \varepsilon_2 v + u = 0.$$

The matrix Λ is thus

$$\Lambda_{\varepsilon_1,\varepsilon_2} = \begin{bmatrix}\varepsilon_1 & -1\\ 1 & \varepsilon_2\end{bmatrix}$$

in which skew symmetry is broken by the small, random coefficients ε_1 and ε_2. We apply CNLF over a long time interval:

$$\frac{u^{n+1}-u^{n-1}}{2\Delta t}+10^4\frac{u^{n+1}+u^{n-1}}{2}+\varepsilon_1 u^n - v^n = 0,$$
$$\frac{v^{n+1}-v^{n-1}}{2\Delta t}+10^{-4}\frac{v^{n+1}+v^{n-1}}{2}+\varepsilon_2 v^n + u^n = 0,$$

with starting conditions $u^0 = v^0 = 1$. We test:

- For $\Delta t = 1.01 > 1$ and $\varepsilon_1 = \varepsilon_2 = 0$ CNLF is unstable. Figure 1 (left) verifies that the instability once again occurs in only the unstable mode.
- For $\Delta t = 0.99 < 1$ and $\varepsilon_1 = \varepsilon_2 = 0$, all modes are stable over a long-time interval, as seen in Figure 1 (right).
- For $\varepsilon_1 = \varepsilon_2 = 10^{-4}$, both modes remain stable for $\Delta t = 0.99$ (Figure 2 left), while neither of them is stable if the perturbation is increased to $\varepsilon_1 = \varepsilon_2 = 10^{-3}$ (Figure 2 right).

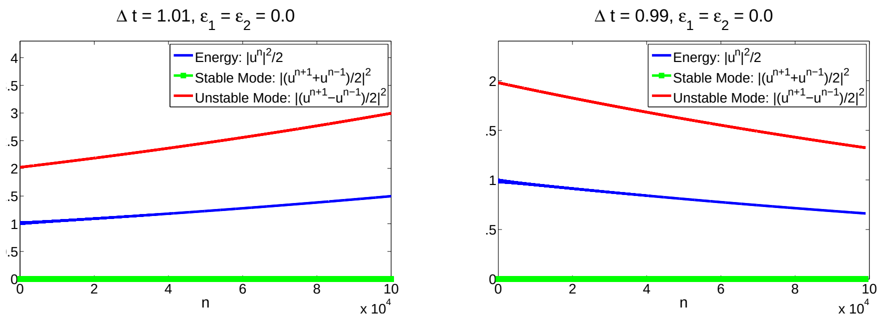

FIGURE 1. For $\varepsilon_1 = \varepsilon_2 = 0$ the unstable mode grows and the stable mode decays for $\Delta t = 1.01$ (left), while for $\Delta t = 0.99$ (right) both modes decay.

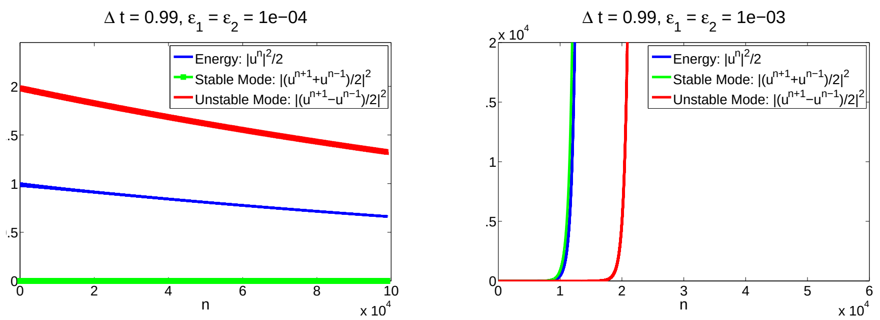

FIGURE 2. For $\Delta t = 0.99$ both modes are stable for $\varepsilon_1 = \varepsilon_2 = 10^{-4}$ (left), while for $\varepsilon_1 = \varepsilon_2 = 10^{-3}$ (right) both modes are unstable.

The instability in the last case may be due to the fact that the perturbation is larger than the smallest eigenvalue of the SPD matrix A. Indeed, we found empirically that the scheme is stable (unstable) when the perturbation is smaller (bigger) than each eigenvalue of the matrix A. If the perturbation is larger than the minimum eigenvalue of the matrix A, then the scheme can possibly become unstable even when the time step condition is satisfied. We see that when the CFL condition is slightly violated (Figure 1 (left)), *instability occurs in the unstable mode* (as reported in practice). When skew symmetry is broken by a large enough factor, instability occurs in all modes (Figure 2 (right)).

5. Conclusions

It has been reported that the CNLF method possesses a weak instability in simulations of complex problems. In practical simulations, stabilizing techniques, e.g., time filters, are used to control the unstable mode of CNLF. A better understanding of this weak instability can be useful downstream for understanding and improving the action of these time filters. In this article, we prove that under the time step condition (2), the unstable mode is indeed asymptotically stable for general autonomous systems. Root conditions provide only necessary stability conditions for the system case, unless the matrices A and Λ commute. Thus, the proof was necessarily based on energy methods. The weak instability of CNLF, we conjecture, is possibly due to the perturbation of the skew symmetric matrix Λ because of the error in numerical integration, computer arithmetic, function evaluation, etc. Indeed, we observe the instability in the numerics when the magnitude of the perturbation is higher than the eigenvalue of the SPD matrix A. We note that the difference in control of the two modes offered by the Crank-Nicolson method has been used in a different context in [9].

References

[1] U. Asher, S. Ruuth and B. Wetton, Implicit-Explicit methods for time dependent partial differential equations, SIAM J. Numer. Anal., 32 (1995) 797-823.
[2] R.A. Asselin, Frequency filter for time integration, Mon. Wea. Rev., 100 (1972) 487-490.
[3] J. Connors and A. Miloua, Partitioned time discretization for parallel solution of coupled ODE systems, BIT Numer. Math., 57 (2011) 253-273.
[4] M. Crouzeix, Une méthode multipas implicite-explicite pour l'approximation des équationes d'évolution paraboliques, Numer. Math., 35 (1980) 257-276.
[5] D.R. Durran, Numerical methods for fluid dynamics with applications to geophysics, Second Edition, Springer, Berlin, 2010.
[6] J. Frank, W. Hundsdorfer and J. Verwer, On the stability of implicit-explicit linear multistep methods, Appl. Numer. Math., 25 (1997) 193-205.
[7] W. Hundsdorfer and S.J. Ruuth, IMEX extensions of linear multistep methods with general monotonicity and boundedness properties, JCP., 225 (2007) 2016–2042
[8] W. Hundsdorfer and J. Verwer, Numerical solution of time dependent advection diffusion reaction equations, Springer, Berlin, 2003.
[9] R. Ingram, A new linearly extrapolated Crank-Nicolson time-stepping scheme for the Navier-Stokes equations, Math. Comp., 82 (2013) 1953-1973.
[10] C. Jablonowski, and D. Williamson, The pros and cons of diffusion, filters and fixers in atmospheric general circulation models, pp. 381–493 in: P.H. Lauritzen, C. Jablonowski, M. Taylor, R.D. Nair (eds.) Numerical Techniques for Global Atmospheric Models, LN in CSE, vol. 80, Springer, Berlin 2011.
[11] O. Johansson and H.-O. Kreiss, Über das Verfahren der zentralen differenzen zur Lösung des Cauchy-problems fur partielle Differentialgleichungen, BIT (Nordisk Tidskr. Informations-Behandling) 3 (1963) 97-107.
[12] E. Kalnay, Atmospheric Modeling, data assimilation and predictability, Cambridge Univ. Press, Cambridge, 2003.
[13] M. Kubacki, Uncoupling Evolutionary Groundwater-Surface Water Flows Using the Crank-Nicolson Leapfrog Method, Numer. Methods Partial Differential Equations, 29 (2012) 1192–1216.
[14] W. Layton, M. Sussman and A. Takhirov, Instability of Crank-Nicolson Leap-Frog for Non-autonomous Systems, Int. J. Numer. Anal. Model. Ser. B, 5 (2014) 289-298.

[15] W. Layton and C. Trenchea, Stability of two IMEX methods, CNLF and BDF2-AB2, for uncoupling systems of evolution equations, Appl. Numer. Math., 62 (2012), 112-120.
[16] Y. Li and C. Trenchea, A higher-order Robert–Asselin type time filter, JCP, 259 (2014), 23–32.
[17] K. Michael, and A.J. Robert, A semi-implicit scheme for grid point atmospheric models of the primitive equations, Mon. Wea. Rev., 99 (1971) 32-36.
[18] A. Robert, The integration of a spectral model of the atmosphere by the implicit method, Proc. WMO/IUGG Symposium on NWP, Japan Meteorological Agency, Tokyo, Japan (1969) 19-24.
[19] S.J. Thomas and R.D. Loft, The NCAR spectral element climate dynamic core: Semi-Implicit Eulerian formulation, J. Sci. Comput., 25 (2005) 307-322.
[20] J.M. Varah, Stability restrictions on a second order, three level finite difference schemes for parabolic equations, SIAM J. Numer. Anal., 17 (1980) 300-309.
[21] J. Verwer, Convergence and component splitting for the Crank-Nicolson Leap-Frog integration method, CWI report 2009, http://oai.cwi.nl/oai/asset/13678/13678D.pdf.
[22] P.D. Williams, The RAW Filter: An Improvement to the Robert–Asselin Filter in Semi-Implicit Integrations, Mon. Wea. Rev., 139 (2011) 1996–2007.
[23] H. Zhang, A. Sandu and S. Blaise, Partitioned and Implicit-Explicit General Linear Methods for Ordinary Differential Equations, J. Sci. Comput., 61 (2014), 119-144.

Department of Mathematics, University of Pittsburgh, Pittsburgh, PA 15217, USA
E-mail: ndh12@pitt.edu and wjl@pitt.edu and yol34@pitt.edu and mam328@pitt.edu
URL: http://www.pitt.edu/∼wjl/ and http://www.pitt.edu/∼mam328/